# Magnetic Properties of Hexanuclear Lanthanide(III) Clusters Incorporating a Central μ 6 -Carbonate Ligand Derived from Atmospheric CO 2 Fixation

**ARTICLE** *in* INORGANIC CHEMISTRY · MARCH 2012

Impact Factor: 4.76 · DOI: 10.1021/ic3002724 · Source: PubMed



**3 AUTHORS:**

Stuart K Langley
Monash University (Australia)
**65** PUBLICATIONS **1,432** CITATIONS
SEE PROFILE

Boujemaa Moubaraki
Monash University (Australia)
**342** PUBLICATIONS **9,423** CITATIONS
SEE PROFILE

Keith S Murray
Monash University (Australia)
**552** PUBLICATIONS **14,759** CITATIONS
SEE PROFILE

Inorganic Chemistry

Communication

pubs.acs.org/IC

# Magnetic Properties of Hexanuclear Lanthanide(III) Clusters Incorporating a Central $\mu_6$-Carbonate Ligand Derived from Atmospheric $CO_2$ Fixation

Stuart K. Langley, Boujemaa Moubaraki, and Keith S. Murray*

School of Chemistry, Monash University, Clayton, Victoria 3800, Australia

Supporting Information

**ABSTRACT:** Three isostructural hexanuclear lanthanide(III) clusters are reported ($Ln^{III}$ = Gd, Tb, and Dy). The metallic core of each complex displays an unusual arrangement of ions, which is stabilized by a $\mu_6$-carbonate ligand. Magnetic studies show that the $Ln^{III}$ ions in each compound are weakly exchange coupled, with the Tb and Dy analogues displaying single-molecule-magnet behavior.

Coordination/cluster chemistry of lanthanide complexes continues to grow because of the observation that many of these compounds act as single-ion or single-molecule magnets (SIMs and SMMs).[1,2] These observed properties result from the combination of a large magnetic moment with a uniaxial magnetoanisotropy, resulting in a bistable ground state. This has most commonly been observed in lanthanides for terbium(III) and dysprosium(III) complexes.[1,2] For mononuclear lanthanide complexes, SIM behavior is attributed to the crystal-field splitting of the lowest $J$ multiplet in such a way that the ground-state $m_J$ value should be doubly degenerate and of high magnitude as well as substantially separated from the next excited state.[3] For polynuclear lanthanide clusters in which the exchange coupling is weak, the SMM properties are still strongly based on the SIM behavior. The exchange interaction is, however, likely to have some effect on the relaxation process,[4] but the mechanism of such a slow relaxation of the magnetization for mono- and multinuclear systems is an active topic for debate.[5] A number of recently reported polynuclear lanthanide clusters have been shown to display very large anisotropy barriers[6] and/or multiple relaxation processes.[7] Therefore, we aim to develop synthetic methodologies for acquiring molecular complexes that display a slow relaxation of magnetization and thus allow us to investigate the relaxation dynamics of lanthanide aggregates. With this in mind, we have undertaken a program for which the goal is the synthesis and magnetic characterization of novel polynuclear lanthanide clusters. Ligands such as triethanolamine ($teaH_3$) and 6-chloro-2-hydroxypyridine (Hchp) have been successfully utilized in the isolation of many d-block transition-metal clusters.[8,9] We have recently isolated several polynuclear lanthanide(III) complexes with the $teaH_3$ ligand and probed their magnetic behavior.[10] To further this chemistry, we have adopted a mixed-ligand approach via the reactions of $teaH_3$ with a variety of coligands, in this case with Hchp. The reaction of $Ln(NO_3)_3{\cdot}6H_2O$ (Ln = Gd, Tb, and Dy), $teaH_3$, and Hchp in a methanolic solution led to the isolation of colorless plates after slow evaporation over 2−5 days. This resulted in three novel isostructural hexanuclear lanthanide clusters of the general formula $[Ln^{III}_6(teaH)_2(teaH_2)_2(CO_3)(NO_3)_2(chp)_7(H_2O)](NO_3){\cdot}4.5MeOH{\cdot}1.5H_2O$ [Ln = Gd (**1**), Tb (**2**), and Dy (**3**); see the Supporting Information (SI) for full experimental details].

Compounds **1**−**3** (**3** is shown in Figure 1, with **1** and **2** shown in Figure S1 in the SI) crystallize in the triclinic space group $P\bar{1}$, with the asymmetric unit containing the entire cluster as well as a nitrate counterion and MeOH and $H_2O$ solvent molecules. It was found that the entirety of two of the pyridonate ($chp^-$) ligands, indicated by O25′ and O28 in Figure 1, is partially occupied, each at 50% occupancy. When a $chp^-$ ligand is absent, a $H_2O$ molecule is found to be coordinated to the appropriate metal ion (see the CIF files in the SI for full details). Hence, over these two sites, there is a total of one $chp^-$ ligand and one $H_2O$ molecule present. Each cluster is

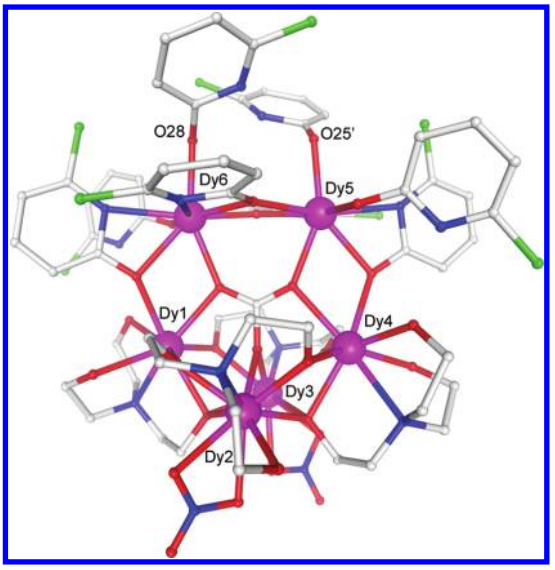


**Figure 1.** Structure of **3**. H atoms and solvent molecules are omitted for clarity. Color code: $Dy^{III}$, purple; O, red; N, blue; C, white; Cl, green. The chp ligands as indicated by O28 and O25′ are at 50% occupancy; see the text for details. See Figures S2−S4 in the SI for the thermal ellipsoid.

**Received:** February 6, 2012
**Published:** March 13, 2012

   dx.doi.org/10.1021/ic3002724 | *Inorg. Chem.* 2012, 51, 3947−3949

isostructural, and **3** will be described here. The complex consists of six $Dy^{III}$ ions, with the metallic core displaying an unusual motif. It may best be described as four coplanar $Dy^{III}$ ions (Dy1, Dy4, Dy5, and Dy6) forming a trapezoid, with the final two ions (Dy2 and Dy3) lying above and below the plane of the longest rectangular edge (Figure 2, left). It was found

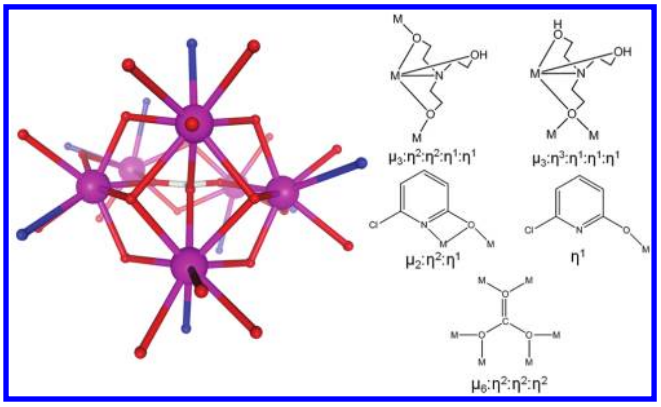


**Figure 2.** (left) Side view of compounds **1**–**3**. (right) Ligand bonding modes observed.

that at the center of the cluster lies a carbonate ion, which adopts a $\mu_6$:$\eta^2$:$\eta^2$:$\eta^2$-bonding mode, binding to all ions present, and it appears to be directing the positions of these ions. Interestingly, a growing number of clusters have been seen to encapsulate $CO_3^{2-}$ ions in the absence of carbonate addition. Recent examples are observed for $Dy_8$,[11] $Dy_6$,[12] and $Dy_4$[13] complexes. The carbonate ion is presumably derived from the fixation of atmospheric $CO_2$ and has attracted interest because of the novel coordination complexes formed. Following the fortuitous atmospheric fixation in the present case and the examples mentioned above, others have now deliberately added sources of carbonate, as well as utilizing methods such as bubbling $CO_2$ through the solution to form novel clusters, such as $Ln_{13}$ complexes.[14] In the present case, the identification of the $CO_3^{2-}$ ion (vs $NO_3^-$) was determined via charge balance and careful consideration of the X-ray diffraction data. Each complex also exhibits carbonate-related IR absorption bands at ~1440 and 845 $cm^{-1}$, as seen for carbonato complexes of other metal ions.[15] The conversion of $CO_2$ to $CO_3^{2-}$ may be similar to the mechanism of carbonic anhydrase. In this case, it involves the nucleophilic attack of hydroxo species bound to the Ln ions in basic conditions to the electrophilic C atom of $CO_2$. This then remains bound to the metal ion, and it is apparent that the carbonate core appears critical to the formation of the cluster. Further work is needed to fully determine the precise mechanism of formation.

Around the periphery of the carbonate-stabilized inorganic core lies the organic shell, which is made up of singly and doubly deprotonated $teaH_3$ ligands, as well as pyridonate, nitrate, and $H_2O$ ligands. These ligands are compartmentalized within the complex, with all seven pyridonate ligands lying at the "top" of the cluster (Figure 1). These display two modes of bonding: four display the $\mu_2$:$\eta^2$:$\eta^1$ coordination mode, while three lie terminal, bonding through a single O atom. All of the pyridonate ligands bridge or lie terminal, coordinating to Dy5 and Dy6, with two of these ligands also then bridging to Dy4 and Dy1. The "bottom" part of the cluster is exclusively bridged via two $teaH^{2-}$ and two $teaH_2^-$ ligands. The $teaH^{2-}$ ligands display the $\mu_3$:$\eta^2$:$\eta^2$:$\eta^1$:$\eta^1$ bonding mode, while $teaH_2^-$ display the $\mu_3$:$\eta^3$:$\eta^1$:$\eta^1$:$\eta^1$ mode. Two nitrate ions then lie terminally chelating to Dy2 and Dy3. All of the bonding modes within **1**–**3** are highlighted in Figure 2 (right). Dy1 and Dy4 are eight-coordinate with distorted square-antiprismatic geometries, with a $\{DyO_7N\}$ coordination sphere. Dy5 and Dy6 display the same geometry but with a $\{DyO_6N_2\}$ coordination environment. Dy2 and Dy3 are nine-coordinate with tricapped trigonal-prismatic geometries, with a $\{DyO_8N\}$ coordination sphere. Average $Ln^{III}$–L (eight-coordinate) bond lengths for **1**–**3** are 2.43, 2.41, and 2.40 Å, respectively, with average $Ln^{III}$–L (nine-coordinate) bond lengths of 2.46, 2.44, and 2.43 Å for **1**–**3**, respectively. There are intermolecular hydrogen bonds formed between the cluster and the various solvent and counterion molecules via the protonated H atoms of the $teaH^{2-}$ and $teaH_2^-$ ligands. Selected bond lengths are given in Table S1 in the SI.

**Magnetic Studies.** Direct-current (dc) magnetic susceptibility measurements were carried out on polycrystalline samples of **1**–**3**, in the 300–2 K temperature range, and in applied magnetic fields of 1, 0.1, and 0.01 T. Plots of $\chi_M T$ versus $T$ are given in Figure 3. Compound **1** $\{Gd_6\}$ displays a

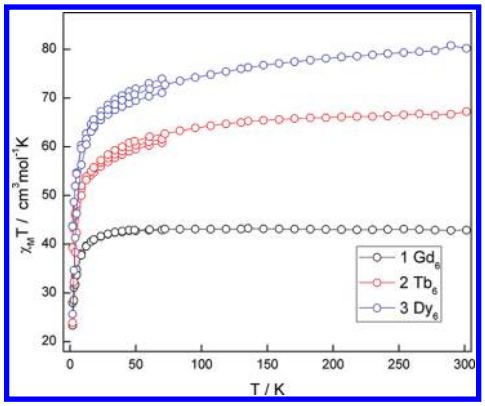


**Figure 3.** Plots of $\chi_M T$ versus $T$ for complexes **1** (bottom), **2** (middle), and **3** (top) measured at 1 T (2–300 K) and 0.1 and 0.01 T (2–70 K). The solid lines are guides for the eye.

room temperature value of 42.90 $cm^3$ $mol^{-1}$ K, which is consistent with the presence of six noninteracting $S = {}^7/_2$ centers (47.25 $cm^3$ $mol^{-1}$ K; $g = 2$). The values remain constant upon a decrease of the temperature to ~10 K, below which a sharp decrease is then seen, with a value of 23.34 $cm^3$ $mol^{-1}$ K found at 2 K, in the field 1 T. There is no field dependence in $\chi_M T$ below 70 K. The data suggest that weak intracluster antiferromagnetic coupling is occurring. It was not possible because of the complexity of the molecule, however, to fit the susceptibility data to calculate $J$ values for the present core bridging geometry. Compounds **2** and **3** display room temperature $\chi_M T$ values of 67.2 and 80.2 $cm^3$ $mol^{-1}$ K, respectively, again consistent with the presence of six noninteracting Tb ($S = 3$, $L = 3$, $^7F_6$, $g = {}^3/_2$, $C = 11.82$ $cm^3$ $mol^{-1}$ K) and Dy ($S = {}^5/_2$, $L = 5$, $^6H_{15/2}$, $g = {}^4/_3$, $C = 14.17$ $cm^3$ $mol^{-1}$ K) centers. The $\chi_M T$ values gradually decrease upon lowering of the temperature, before a more abrupt decrease below 10 K. This is due to depopulation of the $m_J$ sublevels of the $J$ ground state and possibly weak antiferromagnetic interactions. The $M$ versus $H/T$ data at different fields show a rapid increase of the magnetization at low fields, reaching values of 29.66 and 30.37 N$\beta$ at 2 K and 5 T for **2** and **3**, respectively (Figures S5 and S6 in the SI). The non-


dx.doi.org/10.1021/ic3002724 | Inorg. Chem. 2012, 51, 3947–3949

superimposed curves confirm the presence of anisotropy and/or low-lying excited states, which is expected for compounds containing $Tb^{III}$ and $Dy^{III}$ ions. Solid-state alternating-current (ac) susceptibility measurements were performed on compounds **2** and **3** under a zero applied dc field and a small ac field (5 Oe), to check for any SMM behavior. Plots of $\chi_M''$ versus $T$ for **2** and **3** are shown in Figure S7 in the SI and Figure 4, respectively. The out-of-phase susceptibility ($\chi_M''$)

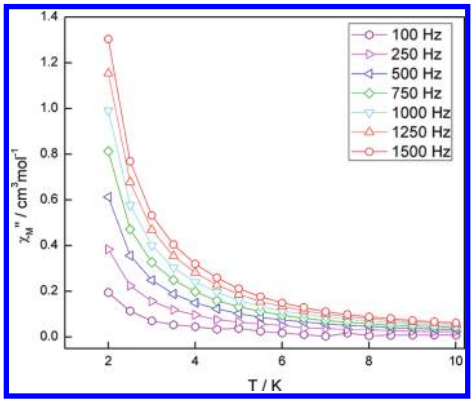


**Figure 4.** Plot of $\chi_M''$ versus $T$ for complex **3**. $H_{dc} = 0$.

displays frequency-dependent "tails" at low temperatures for both compounds, which is suggestive of the presence of slow relaxation of the magnetization, typical of SMM behavior. The peak maxima, however, are to be found below the minimum operating temperature or the maximum frequency of our SQUID instrument. An estimation of the barrier sizes ($E_a$) for **2** and **3** revealed values of ~4.8 and ~3.8 K, with characteristic times ($\tau_o$) of $1.43 \times 10^{-6}$ and $7.89 \times 10^{-6}$, respectively (see Figure S8 in the SI for full details). The barrier sizes observed here are small with respect to the record value for a polynuclear lanthanide species of 528 K.[6b] The absence of any frequency-dependent peaks may be due to fast zero-field quantum tunneling. Hence, ac susceptibility measurements under applied dc fields were performed in order to suppress any possible tunneling effects. Compound **2** now displays an increase in $\chi_M''$ below 10 K in a 5000 Oe field (Figure S9 in the SI), with a plateau found between 2.5 and 4.5 K, before a second increase below 2.5 K. There is still no resolvable maximum observed however. In the case of **3**, nonzero values in $\chi_M''$ are still observed in 5000 (Figure S10 in the SI) and 10000 Oe (Figure S11 in the SI) dc fields but differ from the zero-field measurements, with a broad increase occurring from ~10 K and again still with no clear maxima. There also appears to be a more rapid increase at the lowest temperatures measured. These results suggest that quantum tunneling is likely still active and with the possibility of further relaxation pathways becoming observable, not uncommon in polynuclear systems with several different coordination environments for the $Ln^{III}$ ions present.[16] Again further work is required to determine exactly the mechanisms for slow relaxation in these types of systems.

In summary, a new hexanuclear cluster type for lanthanide compounds has been prepared through the assembly of Ln ions and the ligands $teaH_3$ and Hchp. The center of the cluster contains a $\mu_6$-carbonate ligand, which is derived from atmospheric $CO_2$ fixation. Magnetic studies indicate that weak coupling is present and antiferromagnetic in the case of **1** $\{Gd_6\}$. Compounds **2** $\{Tb_6\}$ and **3** $\{Dy_6\}$ display features typical of SMM behavior. Further work will involve ab initio calculations on **2** and **3** to give anisotropy axes and $J$ values.[4c,7]

## ■ ASSOCIATED CONTENT

### Ⓢ Supporting Information

Experimental, X-ray, bond-length, and magnetic data for **1**−**3** and X-ray crystallographic data in CIF format (CCDC 859103−859105). This material is available free of charge via the Internet at http://pubs.acs.org.

## ■ AUTHOR INFORMATION

### Corresponding Author

*E-mail: keith.murray@monash.edu.

### Notes

The authors declare no competing financial interest.

## ■ ACKNOWLEDGMENTS

We thank the Australian Research Council for financial support.

## ■ REFERENCES

(1) Ishikawa, N.; Sugita, M.; Ishikawa, T.; Koshihara, S.; Kaizu, Y. *J. Am. Chem. Soc.* **2003**, *125*, 8694.

(2) (a) Rhinehart, J. D.; Feng, M.; Evans, W. J.; Long, J. R. *J. Am. Chem. Soc.* **2011**, *133*, 14236. (b) Rhinehart, J. D.; Feng, M.; Evans, W. J.; Long, J. R. *Nat. Chem.* **2011**, *3*, 538. (c) Sessoli, R.; Powell, A. *Coord. Chem. Rev.* **2009**, *253*, 2328.

(3) (a) Rhinehart, J. D.; Long, J. R. *Chem. Sci.* **2011**, *2*, 2078. (b) Sorace, L.; Benelli, C.; Gatteschi, D. *Chem. Soc. Rev.* **2011**, *40*, 3092.

(4) (a) Layfield, R. A.; McDouall, J. J. W.; Sulway, S. A.; Tuna., F.; Collison, D.; Winpenny, R. E. P. *Chem.—Eur. J.* **2010**, *16*, 4442. (b) Sulway, S. A.; Layfield, R. A.; Tuna, F.; Wernsdorfer, W.; Winpenny, R. E. P. *Chem. Commun.* **2012**, *48*, 1508. (c) Long, J.; Habib, F.; Lin, P.-H.; Korobkov, I.; Enright, G.; Ungur, L.; Wernsdorfer, W.; Chibotaru, L.; Murugesu, M. *J. Am. Chem. Soc.* **2011**, *133*, 5319.

(5) Guo, Y.-N.; Xu, G.-F.; Guo, Y.; Tang, J. *Dalton Trans.* **2011**, *40*, 9953.

(6) (a) Hewitt, I. J.; Tang, J.; Madhu, N. T.; Anson, C. E.; Lan, Y.; Luzon, Y.; Etienne, M.; Sessoli, R.; Powell, A. K.. *Angew. Chem., Int. Ed.* **2010**, *49*, 6352. (b) Blagg, R. J.; Muryn, C. A.; McInnes, E. J. L.; Tuna, F.; Winpenny, R. E. P. *Angew. Chem., Int. Ed.* **2011**, *50*, 6530. (c) Blagg, R. J.; Tuna, F.; McInnes, E. J. L.; Winpenny, R. E. P. *Chem. Commun.* **2011**, *47*, 10587.

(7) Lin, P. H.; Burchell, T. H.; Ungur, L.; Chibotaru, L. F.; Wernsdorfer, W.; Murugesu, M. *Angew. Chem., Int. Ed.* **2009**, *48*, 9489.

(8) Langley, S. K.; Moubaraki, B.; Berry, K. J.; Murray, K. S. *Dalton Trans.* **2010**, *39*, 4848.

(9) Langley, S. K.; Helliwell, M.; Sessoli, R.; Teat, S. J.; Winpenny, R. E. P. *Inorg. Chem.* **2008**, *47*, 497.

(10) Langley, S. K.; Moubaraki, B.; Forsyth, C. M.; Gass, I. A.; Murray, K. S. *Dalton Trans.* **2010**, *39*, 1705.

(11) Tian, H.; Zhao, L.; Guo, Y.-N.; Guo, Y.; Tang, J.; Liu, Z. *Chem. Commun.* **2012**, *48*, 708.

(12) Tian, H.; Guo, Y.-N.; Zhao, L.; Tang, J.; Liu, Z. *Inorg. Chem.* **2011**, *50*, 8688.

(13) Gass, I. A.; Moubaraki, B.; Langley, S. K.; Batten, S. R.; Murray, K. S. *Chem. Commun.* **2012**, *48*, 2089.

(14) Chesman, A. S. R.; Turner, D. R.; Moubaraki, B.; Murray, K. S.; Deacon, G. B.; Batten, S. R. *Chem.—Eur. J.* **2009**, *15*, 5203.

(15) Liang, X.; Parkinson, J. A.; Parsons, S.; Weishaupl, M.; Sadler, P. J. *Inorg. Chem.* **2002**, *41*, 4539.

(16) Lin, P.-H.; Sun, W.-B.; Yu, M.-F.; Li, G.-M.; Yan, P.-F.; Murugesu, M. *Chem. Commun.* **2011**, *47*, 10993.